Colloid Polym Sci 275:181–186 (1997)

SHORT COMMUNICATION

G.J. Vancso
G. Liu
J. Karger-Kocsis
J. Varga

AFM imaging of interfacial morphologies in carbon-fiber reinforced isotactic polypropylene

Received: 25 June 1996
Accepted: 17 October 1996

Dr. G.J. Vancso (✉) · G. Liu
University of Twente
Faculty of Chemical Technology
P.O. Box 217
7500 AE Enschede, The Netherlands

J. Karger-Kocsis
Institut für Verbundwerkstoffe GmbH
Universität Kaiserslautern
Postfach 30 49
67663 Kaiserslautern, Germany

J. Varga
Technical University of Budapest
Department of Plastics and Rubber
P.O. Box 92
1521 Budapest, Hungary

Abstract The morphology of high-modulus carbon-fiber (HM-CF) reinforced isotactic polypropylene (iPP) was investigated for the first time by atomic force microscopy (AFM) using chemically etched specimens. The images exhibited α-transcrystalline morphology for samples crystallized from quiescent melts, nucleated by HM-CF. In melts sheared by fiber pulling, αβ-cylindritic columnar morphology was observed in agreement with earlier thermo-optical studies. AFM images in the interfacial region of the β-cylindrites unveiled fine morphological details of α-row nuclei. Based on the observations, we concluded that in β-cylindrites, the lamellar growth in α-row nuclei occurs during epitaxial crystallization on bundles of extended iPP chains which form during shearing of the polymer matrix by fiber pull.

Key words Transcrystallinity – isotactic polypropylene – carbon-fiber – morphology – atomic force microscopy – nucleation

Introduction

Contact between surfaces of solids and crystallizing polymer melts can significantly enhance nucleation density. When there is high nucleation density at the melt–solid interface, the growth of lamellae is restricted in the lateral directions by neighboring entities. The growth direction of such surface nucleated crystals is normal to the surface whereas the polymer chain axis direction is usually parallel with the surface. In such cases, a transcrystalline morphology develops, first described for polymers by Jenckel [1]. Transcrystalline regions can also form when isotactic polypropylene (iPP) crystallizes in contact with graphite and other fibers with α-nucleating ability [2–7].

Fiber-reinforced thermoplastic polymers with transcrystallinity have attracted considerable attention because of their potentially interesting physical properties. The possibility exists that in terms of toughness, resistance to crack propagation, strength, and stiffness, these polymer systems may outperform samples/products made from the pure polymer matrix [8]. Despite extensive research, the exact mechanism of transcrystallization is not clearly understood. It appears that a large variety of parameters may influence the ability of a surface to nucleate transcrystalline growth. For isotactic polypropylene, the influences of fiber type, crystallization temperature, interfacial stress, cooling rate, fiber properties and polymer molar mass have been investigated [3–11]. It was shown by Gray [10] that mechanical stress near the glass–polymer interface in glass fiber containing iPP melt can lead to the formation of transcrystalline-like structures, even when transcrystallization at the surface of quiescent glass fibers was not observed. The supermolecular structure in the vicinity of the sheared layer was found to be rich in β-modification of iPP (β-iPP) [5, 6, 9]. In recent papers, Varga and

Colloid & Polymer Science, Vol. 275, No. 2 (1997)

Karger-Kocsis reported on the results of a thermo-optical study aimed at imaging interfacial morphologies in carbon-fiber reinforced iPP [5, 6]. The results of this work demonstrated that in quiescent melts, α-transcrystalline morphology is induced by high-modulus carbon fibers (HM-CF). In melts sheared by fiber pulling, a polymorphic, columnar morphology can form around the fiber. The growth and structural details of this morphology will depend on the shear, and crystallization, temperatures. The supermolecular structure was reported as being the α form near the fiber–polymer interface. At this interface, an overgrowth of the β-modification was observed for temperatures $T_{\alpha\beta} < T_c \leq T_{pull} < T_{\beta\alpha}$, where $T_{\alpha\beta}$ ($\approx$110 °C) and $T_{\beta\alpha}$ ($\approx$140 °C) are the lower and upper temperature limits of formation of the β-modification [12], T_c is the crystallization temperature, and T_{pull} is the fiber pulling temperature. Varga and Karger-Kocsis suggested a model which explains the formation of this polymorphic structure. The authors assumed that the mechanical stress in the vicinity of the pulled fiber induces the formation of α-row nuclei in the melt. At the surface of these α-row nuclei, it is highly probable that β-nuclei will from (αβ secondary nucleation). Further growth of the front of the α-phase (which originates at the α-row nuclei) will eventually be blocked by β-modification growth (which is initiated by αβ secondary nucleation), due to the higher growth rate of the β-phase. Thus, the α-phase will be confined in the vicinity of the pulled fiber, and will be surrounded by material crystallized in the β-phase. Varga and Karger-Kocsis pointed out in refs. [5, 6] and [11] that while α-transcrystallization involves heterogeneous nucleation at the fiber interface, the formation of cylindritic crystallization cannot be considered to be a heterogeneous nucleation process. In the latter, the growth of the cylindrites is induced by the row-nuclei formed upon mechanical stress, and thus it is a homogeneous nucleation process.

Thermo-optical studies allowed us to identify the α-phase forming at the polymer-HM-CF interface, but, because of limited resolution, morphological details of the α-phase could not be observed. In the present paper, we report on the first atomic force microscopy (AFM) studies of α-transcrystalline and cylindritic morphologies observed in HM-CF reinforced iPP.

Materials

The reinforcement used was a pitch-based, ribbon-like high modulus carbon fiber produced at Clemson University by Prof. D.D. Edie [5]. The isotactic polypropylene (iPP) was of general purpose injection-molding grade (Tipplen H-523, Tisza Chemical Works Ltd, Hungary) with a weight average molar mass of $M_w = 5.2 \times 10^5$ g/mol and a number average molar mass of $M_n = 3.1 \times 10^4$ g/mol. The melt flow index of the polymer was found to be 4 g/10 min at 230 °C and 21.2 N load [1].

Specimen preparation

A single HM carbon fiber was placed between two iPP films and was melted at 220 °C for 5 min. After remelting the sample at 220 °C in a hot stage (Mettler FP82), the specimen was quickly cooled (at a rate of ca. 8 °C/min) to the isothermal crystallization temperature T_c. The carbon fiber was then pulled manually at T_c, always between $T_{\alpha\beta}$ and $T_{\beta\alpha}$. Further details concerning sample preparation have been described in previous papers [5, 6, 11].

In order to study the interface of HM-CF/iPP composites by AFM, the surface of the interfacial region must be exposed to the AFM-probe nanotip. In the present work this was achieved by removing the top layer of iPP with a permanganic etchant [13]. The permanganic etchant solution used consisted of 0.7% w/v of potassium permanganate in a mixture of sulfuric acid (95–97%, Merck) and phosphoric acid (85%, Aldrich) in the volumetric ratio of 2:1. The following etching procedure was applied.

Specimens were etched in 0.7% w/v of the permanganic solution at room temperature typically over 5 h. The etched samples were washed with a diluted sulfuric acid in the volume ratio of 2:7 in distilled water, which was cooled to near the freezing point with ice to prevent the heat of dilution of the original acids from affecting the sample surface. This solution was subsequently decanted. The samples were then washed with hydrogen peroxide (35%) to reduce any remaining manganese dioxide or permanganate. The final step was to wash the sample(s) several times with distilled water, and finally with acetone. An advantage of etching, in addition to "developing" the interface morphology, is that the amorphous matrix is removed much faster than the crystalline component. This will reveal the fine details of the lamellae at the sample surface.

Equipment

A Leitz Dialux 20 polarizing optical microscope, equipped with a Mettler FP 82 hot stage, was used for thermo-optical studies. Optical micrographs were obtained by using crossed polarizers in the usual fashion. Atomic force microscopy (AFM) was performed in the contact mode by using a NanoScope III setup manufactured by Digital Instruments, Santa Barbara, CA, USA. The deflection of the cantilever was kept constant during scanning, i.e., the

height of the specimens is shown in the force microscopy images. Images were taken in air at room temperature using a D-scanner and NanoProbe Si_3N_4 microcantilevers with short, thin legs (100 μm triangular cantilevers with an efffective spring constant of 0.38 N/m). The scanning frequency was 2–3 Hz, and all images shown were captured without the use of image filtering.

Results and discussion

The micrographs in Figs. 1, 2A and 2B, obtained by optical polarizing microscopy, exhibit the basic features of α-transcrystallinity (Fig. 1) and shear induced, row-nucleated cylindritic morphology (Figs. 2A and B).

In Fig. 1, the strong ability of the HM-CF to induce α-transcrystallization in quiescent melts of iPP is evident. Well-developed α-type spherulites in the partially crystallized polymer melt are also visible.

The effect of pulling the HM-CF in the melt, and the subsequent crystallization at the temperature of 135 °C, is shown in Fig. 2A. The features of a typical β-cylindritic morphology grown around the fiber can be clearly seen. It should be mentioned that the crystallization, and the pulling were done at the same temperature, 135 °C, which lies between the $T_{\alpha\beta} \approx 110$ °C and $T_{\beta\alpha} \approx 140$ °C. Within the strongly birefringent β-cylindritic structure, banded areas with low birefringence (arranged cylindrically with the carbon fiber in the axis, at ca. 2/3 of the total radius of the β-cylindrite) indicate the presence of banded lamellae in the β-phase (see Fig. 2A). In Fig. 2A, near the center of the left edge of the micrograph, a highly birefringent β-spherulite is visible. The β-phase in the specimen was selectively "melted out" during heating at a temperature of 158 °C. The resulting morphology is shown in Fig. 2B. The β-spherulite, visible in Fig. 2A at the left edge, as well as the β-overgrowth in the cylindrite, vanished during heating, and only the α-crystalline regions remained unchanged.

As was established earlier [5, 6], the growth of the β-columnar structure in β-cylindrites is induced by secondary $\alpha\beta$-nucleation on α-row nuclei. Following the selective melt-out of the β-phase, the α-phase, in the form of a sawtooth-like pattern at the interface of the HM-CF, is clearly visible in Fig. 2B. It is worthwhile mentioning that hot stage optical and scanning electron microscopy studies of the transcrystalline morphology of iPP in the presence of polyimide (PI) fibers [7] reported on observations of cross-hatched lamellar structures. The morphological architecture depends on the type of fiber used. In this work a model was postulated assuming epitaxial crystallization on regions of the PI fibers containing extended chains.

Due to the limited resolution of optical microscopy, fine morphological details at the fiber–polymer interface

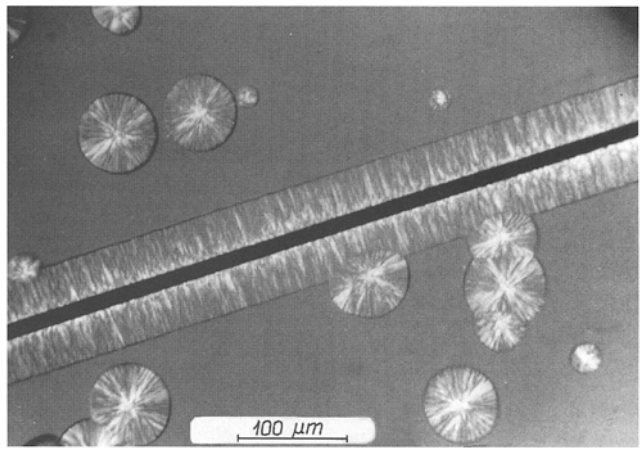

Fig. 1 α-transcrystalline morphology (optical micrograph) induced by a HM carbon fiber in iPP melt at $T_c = 408$ K

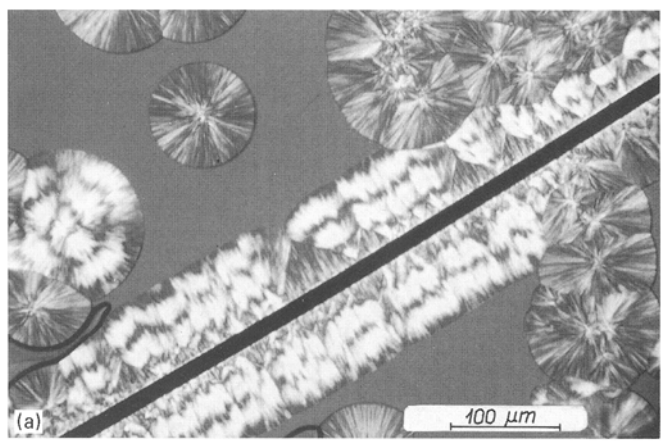

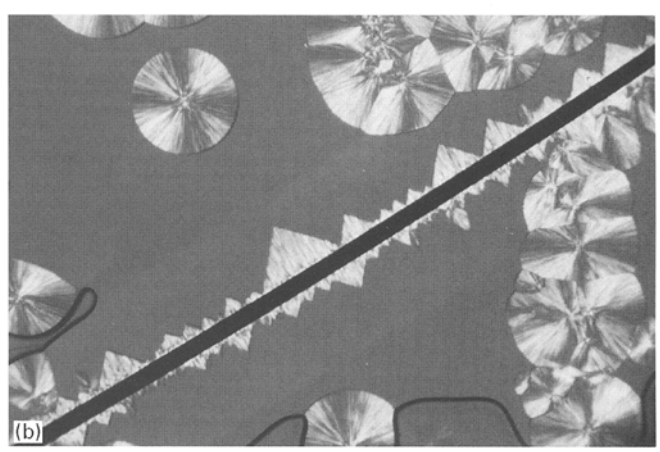

Fig. 2A β-cylindritic morphology (optical micrograph) induced by pulling of a HM-carbon fiber in iPP melt (pulling and crystallization at $T_c = T_{pull} = 408$ K); **B** Same area as shown in Fig. 2A (optical micrograph) after selective melting of the β-phase at $T_f = 431$ K. The "saw-tooth" like α-phase inclusion, which grew on α-row nuclei, is clearly visible

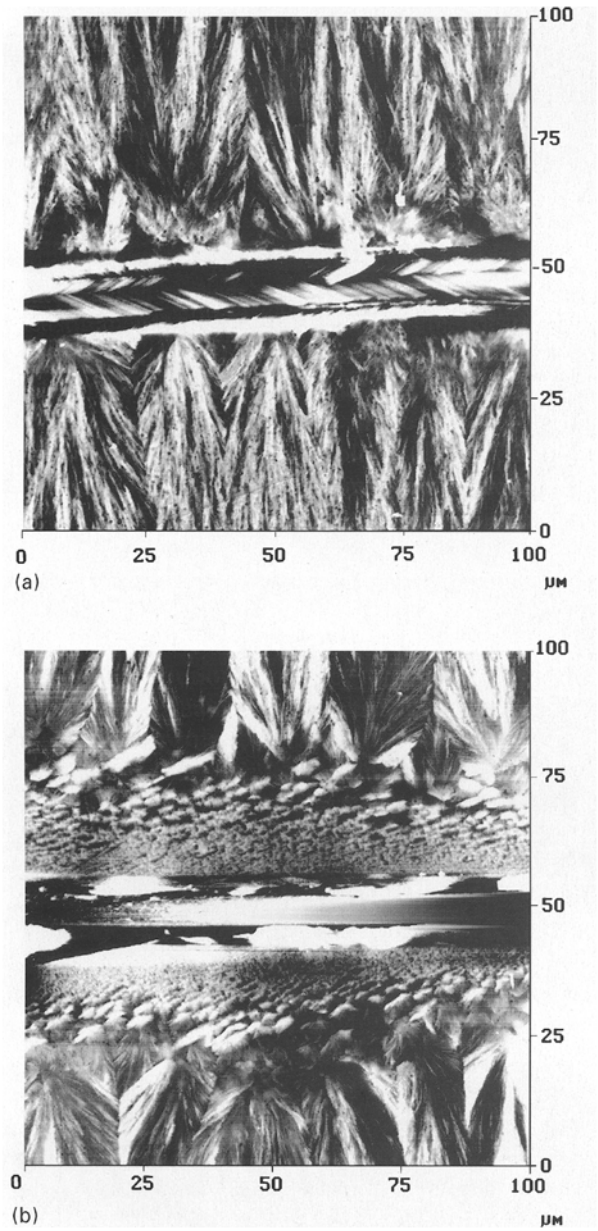

Fig. 3A AFM image of the etched specimen (α-transcrystalline morphology) shown in Fig. 1. Scan size: 100 μm × 100 μm; **B** AFM image of the etched specimen (β-cylindritic morphology) shown in Fig. 2A. Scan size: 100 μm × 100 μm

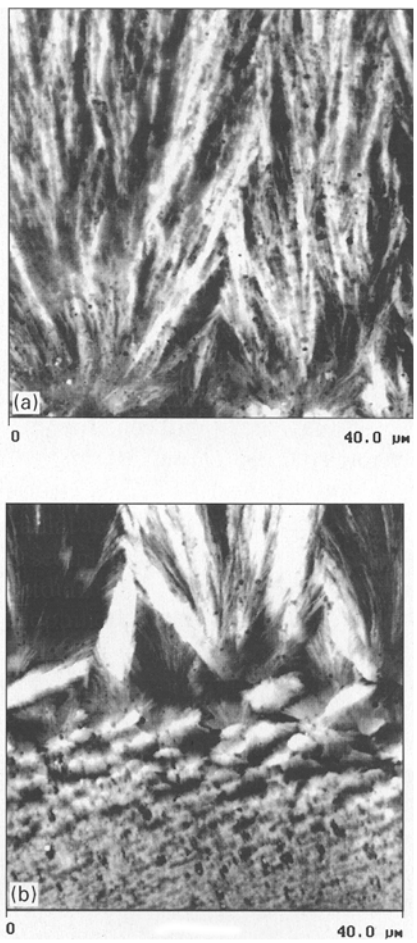

Fig. 4A A close-up of lamellar growth (AFM micrograph) nucleated at the surface of the HM carbon fiber which was used to nucleate α-transcrystalline morphology. The fiber–polymer interface is located near the bottom edge of the image. Scan size: 40 μm × 40 μm; **B** A close-up of α-row nuclei (lower-half) and β-phase lamellae (upper-half) of the β-cylindritic morphology (AFM micrograph) formed at the surface of the HM carbon fiber pulled in the polymer melt. The fiber–polymer interface is located near the bottom edge of the image. Scan size: 40 μm × 40 μm

cannot be captured with high resolution. In previous studies atomic force microscopy [14] was used to study the lamellar morphology of isotropic iPP films [15], as well as the microfibrillar morphology and the polymer architecture of uniaxially stretched iPP rods, the latter with true molecular resolution [16]. In order to study the morphology at the fiber–polymer interface, we performed AFM imaging on the specimens shown in Figs. 1, 2A and B. Prior to imaging, the surfaces of the specimens were etched.

Figures 3A and B display $(100\ \mu m)^2$ scans: Fig. 3A displays the α-transcrystalline morphology, and Fig. 3B shows the β-cylindritic structure. In both cases the fiber is (nearly) horizontal, at ca. $\frac{1}{2}$ height of the image. It is known that AFM is not well suited to image rough surfaces or steep/deep features. During the etching process, "deep" grooves and a rough, uneven surface were formed in the fiber region of the sample, and thus, the corresponding AFM images are inconclusive. Nevertheless, above and below the fiber region, the surface morphology of the samples is clearly visible and well-resolved.

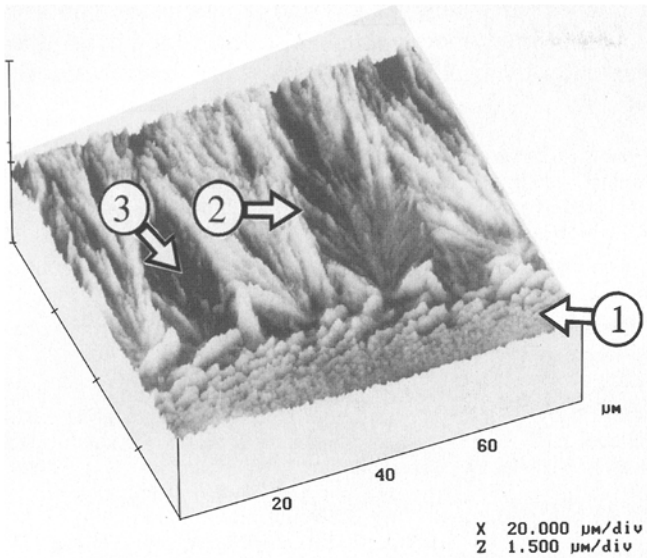

Fig. 5 Surface plot of an AFM image showing true "three-dimensional" topology of the β-phase lamellae and the α-row nuclei in β-cylindritic morphology. One division in the vertical axis corresponds to 1.5 μm. Scan size: 80 μm × 80 μm: (1) α-row nucleated structure; (2) β–α impingement line; (3) α inclusion

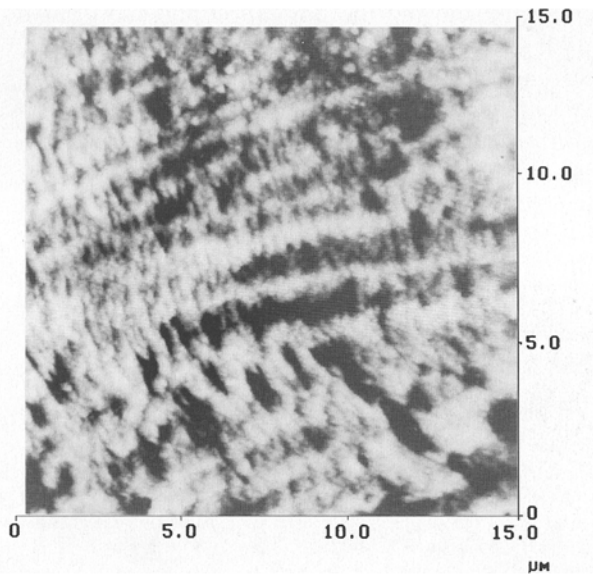

Fig. 6 A close-up of α-row nuclei in a β-cylindritic structure. AFM image, scan size: 15 μm × 15 μm

The basic morphological features observed in Figs. 3A and B are similar to the images obtained by optical microscopy: the lamellar transcrystalline structure originating from the fiber interface is obvious in Fig. 3A (quiescent melt), while features of the β-cylindritic structure can be clearly seen in Fig. 3B. The same structures are shown in Figs. 4A and B, with scans depicting (40 μm)^2 areas near the interface of the fibers. The interface itself is located at the bottom of the micrographs (the fiber itself is not shown). During etching, many scattered, "pock-mark"-like artifacts were formed, probably due to the water content of the acid which was used. These sample preparation artifacts are clearly visible, especially in the α-transcrystalline structures shown in Figs. 3A and 4A.

It must be noted at this juncture that the AFM images shown here cannot be used to identify the crystal phase of the polypropylene imaged. This can, however, be achieved with high-resolution AFM scans, as discussed in ref. [15]. In the present study, evidence for the identification of the phases comes from the birefringence observed in the optical micrographs.

Figure 5 shows a perspective, quasi-three-dimensional surface plot of the β-cylindritic morphology. The vertical scale in this picture corresponds to 1.5 μm per division (as opposed to the 20 μm per division for the horizontal x and y axes), i.e., the surface morphological features are emphasized in the vertical direction. Near the bottom edge (at the fiber–polymer interface), α-row nuclei are depicted. Non-crystallographic branching, and impingement lines in the growth direction within the β-columnar phase, can be clearly seen.

In Fig. 6, we show the interfacial region near the fiber–melt interface with a magnification significantly higher than the resolution limit of optical microscopy (scan size: 15 μm × 15 μm). As has been established earlier, this region contains the α-phase of iPP and corresponds to the α-row nuclei. The shear direction in the melt during the pulling of the HM-CF was nearly horizontal. Clear features at angles between 5° and 15°, i.e. essentially parallel with the shear, can be distinguished in Fig. 6. Overgrowth of lamellar bundles in the shear-perpendicular (nearly veritcal) direction can also be clearly seen. These features, resolved for the first time, yield valuable information regarding the α-row nucleation mechanism.

In the early pioneering work of Keller [17] it was shown that for polyethylene, as a representative example, crystallization under stress results in lamellar crystal growth in directions normal to the direction of the mechanical stress. The alignment and twist of the lamellae, as well as the nucleation density, were found to depend on the stress. The model of Keller was tested and found to be true for other polymers. Therefore, this model can also be applied to the formation of the α-row nuclei depicted in Fig. 6. Based on this model, and on the morphology shown in Fig. 6, it can be postulated that in β-cylindrites, the lamellar growth in α-row nuclei occurs during epitaxial crystallization on bundles of extended PP chains which form during shearing of the polymer matrix by the fiber

Colloid & Polymer Science, Vol. 275, No. 2 (1997)

pull. A scheme showing the nucleation and the growth geometry is given in ref. [6], Fig. 3.

According to this model, the nearly horizontal features in Fig. 6 correspond to underlying bundles of extended chains, on which the overgrowth of twisted lamellae occurs. These lamellae serve as the self-nuclei for β, as well as for α lamellae observed in the β-cylindritic morphology in the vicinity of the fiber. Because the growth of the β-phase at temperatures between $T_{\alpha\beta}$ and $T_{\beta\alpha}$ is faster than the growth of the α-modification [12], the α-modification is eventually phased out (see saw-tooth α-structure in Fig. 2B).

Acknowledgments Financial support given by the University of Twente is greatly appreciated. The authors thank Ms. Sandra de Jonge and Mrs. Anne Klemperer for their help with the preparation of the manuscript.

References

1. Jenckel E, Teege E, Hinrichs W (1952) Kolloid 7, 129:19
2. Hobbs SY (1971) Nature Phys Sci 234:12
3. Thomason JL, van Rooyen AA (1992) J Matter Sci 27:889
4. Avella M, Della Volpe G, Martuscelli E, Raimo M (1992) Polym Eng Sci 32:376
5. Varga J, Karger-Kocsis J (1995) Polymer 36:4877
6. Varga J, Karger-Kocsis J (1996) J Polym Sci Polym Phys Ed 34:657
7. Sukhanova TE, Lednicky F, Urban J, Baklagina G, Mikhailov GM, Kudryavtsev VV (1995) J Mater Sci 30:2201
8. Schoolenberg GE, Van Rooyen AA (1993) Composite Interfaces 1:243
9. Devaux E, Chabert B (1991) Polym Comm 32:464
10. Gray DG (1974) J Polym Sci Polym Lett 12:645
11. Varga J, Karger-Kocsis J (1993) Polym Bull 30:105; Varga J, Karger-Kocsis J (1993) Composite Sci Techn 48:191
12. Varga J (1992) J Mater Sci 27:2557
13. Olley R, Bassett DC (1982) Polymer 23:1707
14. For reviews see: Miles MJ (1994) New techniques in microscopy In Characterization of Solid Polymers (ed) Spells SJ, ch Chapman & Hall, London 1994; Magonov SN, Whangbo MH (1996) Surface Analysis with STM and AFM, VCH, Weinheim
15. Schönherr H, Snétivy D, Vancso GJ (1993) Polym Bull 30:567
16. Snétivy D, Vancso GJ (1994) Polymer 35:461
17. Keller A, Machin MJ (1967) J Macromol Sci (Phys) B1:41